On supplying LEDs from very low dc voltages with high frequency AC-LED drivers

Ignacio Castro, Daniel G. Aller, Manuel Arias, Diego G. Lamar, Marta M. Hernando and Javier Sebastian
Departamento de Ingeniería Eléctrica, Electrónica, de Computadores y Sistemas
University of Oviedo
Gijón 33204, Spain
e-mail: castroignacio@uniovi.es

***Abstract*— This work studies the driving of white Light Emitting Diodes (LEDs) from very low voltages in the range of 1.2 to 2 V. The proposed idea is based on replacing the standard Schottky diode used in conventional converter topologies (i.e., buck, buck-boost and boost) with an LED, while shortcutting the output of the converter. In this configuration, the LED works both as the load and as the rectifier diode of the converter, hence, switching the LED at high frequencies (i.e. > 100 kHz). Moreover, a thorough analytical study is carried out for the two topologies rendered in this work. Particularly emphasizing their static analysis and the obtaining of the boundaries between the different conduction modes. Finally, the idea is validated experimentally by means of the boost converter variation (i.e., DL//S AC-LED driver). The DL//S AC-LED driver has also been compared with a dc-dc boost converter showing a better luminous efficacy while disposing of the Schottky diode and the output capacitor. This analysis is carried out when connected to a Li-Ion battery using a simple control and integrated circuit for its development.**

Keywords*— LED driver, AC-LED driving, Single-cell battery and low input voltages.

I. Introduction

Light Emitting Diodes (LEDs) are increasingly becoming our main source of artificial light in our homes, offices or streets due to their reliability, long life, energy efficiency and low maintenance requirements. It is a well-known fact, that LEDs can only be driven by forward currents, since they behave as a diode allowing the current to flow in one direction only. This fact has made the driving of LEDs from AC grids a main research topic to replace old inefficient luminaries [1], [2]. In fact, if the current source is not acceptable for the driving of the luminaire a dc-dc converter needs to adapt the level of current to drive them accurately.

For the application under study, which is driving a single LED from a very low voltage (i.e., a battery cell whose voltage can vary in the range of 1.2 to 2 V), the dc-dc converter needs to be able to boost the input voltage to an adequate value. This voltage needs to be higher than the knee-voltage of the LED, which is usually around 3 V, for it to start illuminating. Previous literature regards the Joule Thief as the preferred solution for driving LEDs from very low voltages, based on a blocking oscillator circuit [3], [4], due to its low component count and its simple driving. However, the lack of ease to implement a current feedback loop and the low efficiency displayed (i.e. below 80%) are the main drawbacks of this solution. In order to solve these issues, a conventional dc-dc converter can be suitable for this task based on either a boost, see Fig. 1 (a) or a buck-boost converter, see Fig. 1 (c). Nowadays, the use of these topologies is a possibility at the low input voltage of the application due to the newer Pulse Width Modulation (PWM) driving solutions based on micro-power dc-dc converters, which in the case of the boost converter are able to achieve roughly an 88% efficiency at their peak. However, the losses caused by the voltage drop of a conventional PN diode (i.e. typically, from 1 to 1.5 V) will cause the electrical efficiency to plummet. Moreover, using a Schottky diode or active rectification is not a possibility due to the cost restrictions of the application. In fact even when using a Schottky diode, the voltage drop will still be significant (i.e., typically from 0.25 to 0.5 V). Therefore, the proposal of this work is to replace the rectifier diode on traditional dc-dc converters with a white LED, while short-circuiting the output of the converter. As a result, two different converters can be obtained: LED paralleled with Switch (DL//S AC-LED driver, i.e. Fig. 1 (b)) and LED paralleled with Inductor (DL//L AC-LED driver, i.e. Fig. 1 (d). It should be noted, that while in conventional dc-dc converters the LEDs are supplied with a constant current, in the DL//S and DL//L AC-LED drivers, the

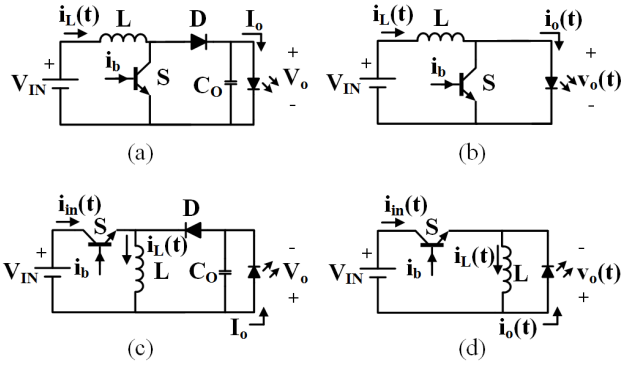

Fig. 1. Basic converters. (a) Boost converter. (b) DL//S AC-LED driver. (c) Buck-boost converter. (d) DL//L AC-LED driver.

This work has been supported by the *Spanish Government* under Project MINECO-17-DPI2016-75760-R and the *Principality of Asturias* under the grants "*Severo Ochoa"* BP14-140 and by the Project SV-PA-17-RIS3-4, and by European Regional Development Fund (ERDF) grants.

978-1-5386-5541-2/18/$31.00 ©2018 IEEE

LED is supplied with a pulsed current, pulsing at the same frequency at which the main switch (i.e., S) is operating. The operation of the LED at high frequencies (i.e., > 100 kHz) acting as the regular diode of a power converter, also referred in literature as high-frequency AC-LED driving, has been studied by means of resonant dual half bridges [6]-[8], a flyback converter working in Discontinuous Conduction Mode (DCM) [9], self-oscillating topologies [10] or quasi-resonant converters [11], [12]. All these works conclude that LEDs are able to switch at high frequencies under different current waveforms. The latest works undergo a reliability analysis that shows that this method can provide a long lifetime on the LEDs as long as the reverse recovery effect is avoided on them [11], [12].

This work explores the possibility of using LEDs as the rectifier diodes of dc-dc converters with the help of the two proposed LED drivers, aiming to avoid the reverse recovery effect by operating in DCM without incurring in increasing the complexity of the LED driver [13], [14]. Furthermore, an analytical study is carried out for both topologies along Section II to understand their advantages and limitations, as well as obtaining their analytical waveforms. Then, the analysis is completed by studying and normalizing the boundaries between Continuous Conduction Mode (CCM) and DCM for both converters. Along Section III, the proposed control methodology is discussed based on the use of a simple IC. In order to elucidate which solution is best, Section IV makes an experimental comparison in terms of luminous efficacy and electrical efficiency between the conventional topologies and the proposed topologies in the different operating modes (i.e., CCM and DCM). Finally, the most important conclusions extracted from this work are discussed in Section V.

II. WORKING PRINCIPLE

As in the conventional dc-dc converters, the proposed topologies are based on a PWM signal that drives the main switch (i.e., S), causing the inductance to magnetize or demagnetize in accordance to a determined duty cycle (i.e., d) that turns on and off the main switch. Taking into account this principle there are three equivalent circuit that each topology undergoes: 1) Transistor conducting, 2) Diode conducting and 3) None of them conducting. The last stage will only appear when operating in DCM, which will be the aim of this work, thus the importance of the last subsection studying the boundaries between CCM and DCM.

A. Static analysis of the DL//S AC-LED driver

From this basic principle, there are three possible equivalent circuits for the DL//S AC-LED driver, which are shown in Fig. 2 considering the equivalent circuit of the LED as the series connection of an ideal diode, an equivalent dynamic resistance (r_{LED}) and an ideal voltage source (V_{γ_LED}).

Magnetizing stage, see Fig. 2 (a), refers to the period of time when the main switch is conducting (i.e., $t < dT_s$), hence linearly charging the inductance in accordance to,

$$i_L(t) = i_{L_{valley}} + \frac{V_{IN}}{L}t, \tag{1}$$

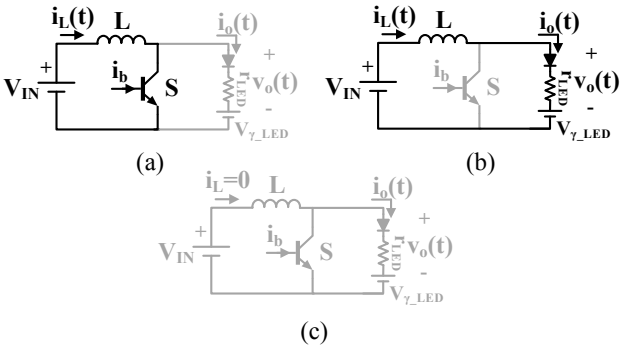

Fig. 2. Equivalent circuits for the DL//S topology. (a) Conduction of the switch. (b) Conduction of the LED (c) No conduction of either switch or LED.

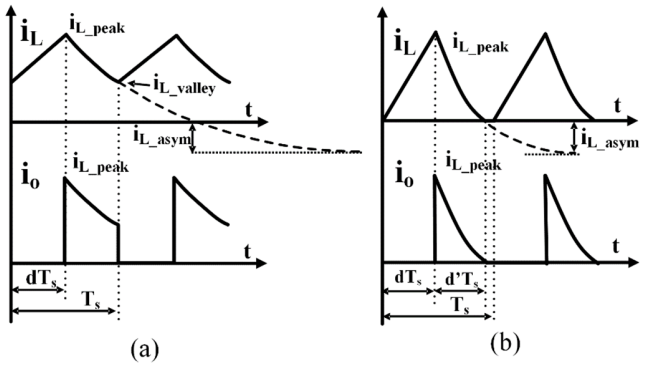

Fig. 3. Most representative waveforms for the DL//S AC-LED driver. (a) CCM (b) DCM.

where V_{IN} is the input voltage, L is the inductance value and i_{L_valley} corresponds to the minimum current through the inductance, as can be seen in Fig. 3 (a). Consequently, during this stage there is no current across the LED. The end of this stage is marked by the turn off of the main switch that will stop conducting, causing L to start demagnetizing through the LED, see Fig. 2 (b).

Demagnetizing stage, see Fig. 2 (b), refers to the period when the inductance demagnetizes as the LED starts conducting. This effect is represented in the current by,

$$i_L(t) = i_{L\_asym} + \left(i_{L\_peak} - i_{L\_asym}\right)e^{-\frac{(t-d\cdot T_S)}{\tau}} \tag{2}$$

where T_s is the switching period and i_{L_asym} is the asymptotic value that the curve tends to, as shown in Fig. 3 (a), τ is the time constant, and i_{L_peak} is the maximum value of the $i_L(t)$. The values taken by i_{L_asym} and τ are,

$$i_{L\_asym} = \frac{V_{IN} - V_{\gamma\_LED}}{r_{LED}}, \tag{3}$$

and,

$$\tau = \frac{L}{r_{LED}}. \tag{4}$$

It is important to note that in this stage the current does not demagnetize linearly as it does in the conventional converters, due to the lack of an output capacitor behaving as a constant voltage source. Consequently depending on the value of r_{LED}.

The duration of this stage is completely reliant on the mode of operation of the converter (i.e., either CCM or DCM). Under CCM operation, its duration will be determined by the duty cycle of the main switch, being the duration (1-d)T_s, whereas for DCM operation its duration will be marked by $i_L(t)$ reaching the zero current value.

For CCM operation, the next condition needs to be fulfilled in steady state:

$$i_L(T_s) = i_{L\_valley}. \tag{5}$$

Then, from this assumption is possible to attain the values of i_{L_valley} and i_{L_peak} as,

$$i_{L\_valley} = \frac{i_{L\_asym}(1 - e^{\frac{(d-1)T_s}{\tau}}) + \frac{V_{IN} d T_s}{L} e^{\frac{(d-1)T_s}{\tau}}}{1 - e^{\frac{(d-1)T_s}{\tau}}}, \tag{6}$$

and,

$$i_{L\_peak} = i_{L\_valley} + \frac{V_{IN}}{L} d T_s. \tag{7}$$

Equations (3), (4), (6) and (7) provide (1) and (2) with the required parameters in order to attain the expressions of $i_L(t)$ and $i_o(t)$ during a switching period. Subsequently, it becomes possible to obtain the average power delivered to the LED within a switching period by integrating the instantaneous power consumed by the LED as,

$$P_{LED} = \frac{1}{T_s} \int_{dT_s}^{T_s} (i_L(t) V_{\gamma\_LED} + i_L(t)^2 r_{LED}) dt, \tag{8}$$

where $i_L(t)$ is defined by (2).

No conduction stage, see Fig. 2 (c), is an optional stage that happens under DCM operation considering that there is no energy left on the inductance to continue on driving the LED. The time duration of this stage can be defined as the time during which the current through the inductance is zero, until the main switch is turned on again, see Fig. 3 (b).

For operation in DCM, the study is rather similar to the one carried out for CCM, and as such, equations (1)-(4) and (7) are valid for this mode. In this scenario the assumption made in steady state is:

$$i_{L\_valley} = 0. \tag{9}$$

It should be noted that in DCM, (2) is only valid during the time interval d'T_s, which is defined as the time the current through the LED is higher than zero, see Fig. 3 (b). Consequently, d' can be calculated by substituting (9) into (2) and solving for d', yielding,

$$d' = \frac{\tau}{T_s} \cdot ln\left(\frac{i_{L\_peak} - i_{L\_asym}}{-i_{L\_asym}}\right). \tag{10}$$

At this point, it is possible to attain the average power delivered to the LED in a similar fashion to CCM operation, as,

$$P_{LED} = \frac{1}{T_s} \int_{dT_s}^{(d'+d)T_s} \left(i_L(t) V_{\gamma\_LED} + i_L(t)^2 r_{LED}\right) dt. \tag{11}$$

TABLE I. VALUES OF THE BASE MAGNITUDES USED IN THE NORMALIZATION

Magnitude	**BASE VALUE**
Time	T_s
Voltage	V_{γ_LED}
Impedance	r_{LED}
Current	$I_{base} = V_{\gamma\_LED}/r_{LED}$
Power	$P_{base} = (V_{\gamma\_LED})^2/r_{LED}$

The boundary between CCM and DCM can be studied by matching d' in (10) to 1-d. Then,

$$1 - d = \frac{L}{T_S \cdot r_{LED}} \cdot ln\left[\frac{d T_s \frac{V_{IN}}{L} - i_{L\_asym}}{-i_{L\_asym}}\right] \tag{12}$$

However, (12) happens to be a transcendental equation, which means that numerical methods are required to study the boundary between the two modes. Considering the difficulties caused by the previous statement, a normalized analysis is carried out in function of some base magnitudes to be able to graphically analyze the conduction mode of the LED driver.

B. Normalized analysis of the DL//S AC-LED driver

In order to normalize the study of the DL//S AC-LED driver it is mandatory to select the base magnitudes to normalize, see Table I. From these base magnitudes is possible to define the next normalized expressions:

$$t_n = \frac{t}{T_s}, \tag{13}$$

$$\tau_n = \frac{\tau}{T_s} = \frac{L}{r_{LED} T_s}, \tag{14}$$

$$V_{Gn} = \frac{V_{IN}}{V_{\gamma\_LED}}, \tag{15}$$

$$i_{Ln}(t) = \frac{i_L(t)}{I_{base}} = \frac{i_L(t) r_{LED}}{V_{\gamma\_LED}}, \tag{16}$$

$$i_{L\_valleyn} = \frac{i_{L\_valley}}{I_{base}} = \frac{i_{L\_valley} r_{LED}}{V_{\gamma\_LED}}, \tag{17}$$

$$i_{L\_peakn} = \frac{i_{L\_peak}}{I_{base}} = \frac{i_{L\_peak} r_{LED}}{V_{\gamma\_LED}}, \tag{18}$$

$$P_{LEDn} = \frac{P_{LED}}{P_{base}} = \frac{P_{LED} r_{LED}}{(V_{\gamma\_LED})^2}. \tag{19}$$

At this point it is possible to consider (3) and (14) equations to rewrite (12) as,

$$d V_{INn} + \tau_n (1 - V_{Gn}) \left(1 - e^{\frac{1-d}{\tau_n}}\right) = 0. \tag{20}$$

Equation (20) depends on multiple parameters. However, most of them are well-known in the design process, such as,

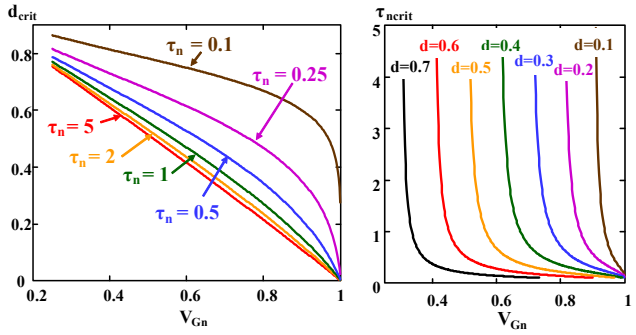

(a) (b)

Fig. 4. Boundary between conduction modes for the DL//S AC-LED driver. (a) d_{crit} versus V_{Gn} and τ_n. (b) τ_n versus d and V_{Gn}.

V_{γ_LED}, r_{LED} and V_{IN}. Therefore, it is only required to study the boundary between CCM and DCM by varying τ_n and d. For that matter, Fig. 4 represents the value of d in the boundary between modes (d_{crit}) for different V_{Gn} and τ_n, see Fig. 4 (a), and for the critical τ_n value (τ_{ncrit}) for different values of V_{Gn} and d, see Fig. 4 (b). The importance of Fig. 4 is such that it helps the designer on selecting the desired operating mode, in accordance to:

- For operation in CCM either d needs to be greater than d_{crit} for given values of V_{Gn} and τ_n, in accordance to Fig. 4 (a), or τ_n needs to be greater than τ_{ncrit} for given values of d and V_{Gn}, in accordance to Fig. 4 (b).
- For operation in DCM either d needs to be lesser than d_{crit} for given values of V_{Gn} and τ_n, in accordance to Fig. 4 (a), or τ_n needs to be lesser than τ_{ncrit} for given values of d and V_{Gn}, in accordance to Fig. 4 (b).

Continuing the normalization process, and considering equations (13)-(19), it is possible to obtain the normalized value of the average P_{LED}, P_{LEDn}. In this particular case (8) and (11) can be unified within a single expression considering that the only difference between the two is the expression of the upper limit of the integral. Therefore,

$$P_{LEDn} = \int_{d}^{d'+d} (i_{Ln}(t) + i_{Ln}(t)^2) dt_n. \tag{21}$$

where d' takes the following values depending on its operating mode:

$$CCM: d' = 1 - d, \tag{22}$$

$$DCM: d' = \tau_n \, ln\left[\frac{\frac{V_{Gn} d}{\tau_n} + 1 - V_{Gn}}{1 - V_{Gn}}\right]. \tag{23}$$

As regards $i_{Ln}(t)$, which is obtained by normalizing (2) with the help of (7), its expression taking into account operation in DCM (i.e., $i_{L\_valley} = 0$) can be defined by,

$$i_{Ln}(t) = V_{Gn} - 1 + \left(i_{L\_valleyn} - V_{Gn} + 1 + \frac{dV_{Gn}}{\tau_n}\right) e^{\frac{(d-t_n)}{\tau_n}}, \tag{24}$$

where $i_{L\_valleyn}$ takes the following values for CCM and DCM operation:

$$CCM: i_{L\_valleyn} = \frac{V_{Gn} - 1 + \left(-V_{Gn} + 1 + \frac{dV_{Gn}}{\tau_n}\right) e^{\frac{(d-1)}{\tau_n}}}{1 - e^{\frac{(d-1)}{\tau_n}}}, \tag{25}$$

$$DCM: i_{L\_valleyn} = 0. \tag{26}$$

At this point of the analysis, it is possible to study the variation of P_{LEDn} when varying V_{Gn}, d and τ_n. Fig. 5 represents this variation, showing how the power given to the LED drastically increases when the DL//S AC-LED driver changes its operating mode from DCM to CCM. It can also be seen how the power transferred to the LED is completely reliant on the parameter τ_n under DCM operation, becoming inconsequential under CCM. This behaviour is identical to any dc-dc converter, where the dc gain depends on d for CCM operation, whereas for DCM it depends on several parameters as are: L, T_s and the load. From these statements, it can be seen that τ_n plays the same role as the dimensionless parameters k (i.e., $k = 2L/(RT_s)$) in the conventional dc-dc converters [15].

C. *Static analysis of the DL//L AC-LED driver*

The analysis carried out for the DL//L AC-LED driver is rather similar to the DL//S AC-LED driver, as it has the same three equivalent circuits, which are depicted in Fig. 6. The most significant change appears on i_{L_asym} which for this AC-LED driver happens to be:

$$i_{L\_asym} = \frac{-V_{\gamma\_LED}}{r_{LED}} = -I_{base}. \tag{27}$$

Consequently, the only equations that change from the previous analysis are (20), (23), (24) and (25), obtaining:

$$dV_{Gn} + \tau_n \left(1 - e^{\frac{1-d}{\tau_n}}\right) = 0, \tag{28}$$

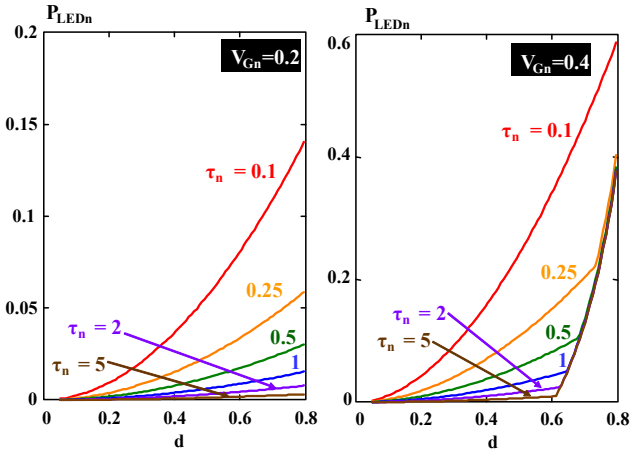

Fig. 5. Normalized average power consumed by the LED in the DL//S LED driver for different values of V_{Gn}, d and τ_n.

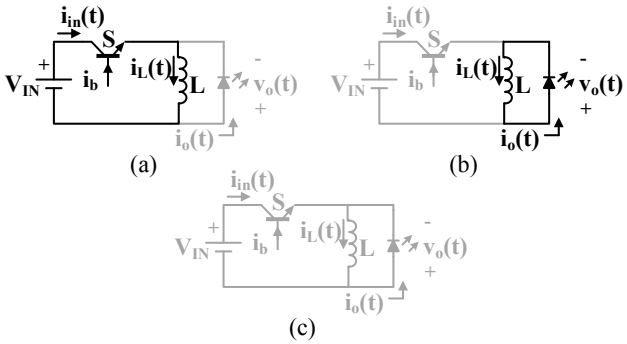

Fig. 6. Equivalent circuits for the DL//L AC-LED driver. (a) Conduction of the switch. (b) Conduction of the LED (c) No conduction of either switch or LED.

$$d' = \tau_n \, ln\left[\frac{dV_{Gn}}{\tau_n} + 1\right], \tag{29}$$

$$i_{Ln}(t) = -1 + \left(i_{L\_valleyn} + 1 + \frac{d \cdot V_{Gn}}{\tau_n}\right) e^{\frac{(d-t_n)}{\tau_n}}, \tag{30}$$

and,

$$i_{L\_valleyn} = \frac{\left(1 + \frac{dV_{Gn}}{\tau_n}\right) \cdot e^{\frac{(d-1)}{\tau_n}} - 1}{1 - e^{\frac{(d-1)}{\tau_n}}}. \tag{31}$$

These expressions complete the analysis on the DL//L AC-LED driver, becoming possible to perform the same graphical representations as those done for the DL//S AC-LED driver in order to study the boundary between conduction modes and the average power transferred by the LED driver to the LED.

The boundary between modes is studied in Fig. 7. It should be noted that the statements introduced for the DL//S AC-LED driver are still valid for this LED driver. In addition, it can be seen in Fig. 7 (a) how the variation of τ_n does not impact the boundary as much as in the previous converter.

Finally, for the DL//L AC-LED driver the power transferred to the LED is studied in Fig. 8 for different values of V_{Gn}, d and τ_n. If these results are compared to those of Fig. 5, it can be seen that the performance of this converter is extremely similar, but it is unable to transfer the same amount of power to the LED for the same values of V_{Gn}, d and τ_n.

III. Proposed Control

One of the key features of using a dc-dc converter to drive LEDs is the ability to control the current supplied to the LEDs using a feedback control loop. In the particular case of the proposed AC-LED drivers, the use of a feedback control loop would require to filter the high frequency current that feeds the LEDs. This will incur into adding more components in the design, which will be undesired. For that matter, the proposal of this work is actually controlling the peak current value on the switch, just like in a peak current mode control (PCMC) [16].

Fig. 9 shows the proposed control particularized for the DL//S AC-LED driver. As can be seen, the current across the main switch is measured and a compensation ramp is added. Then, this voltage is compared to a voltage reference (V_{ref}) that

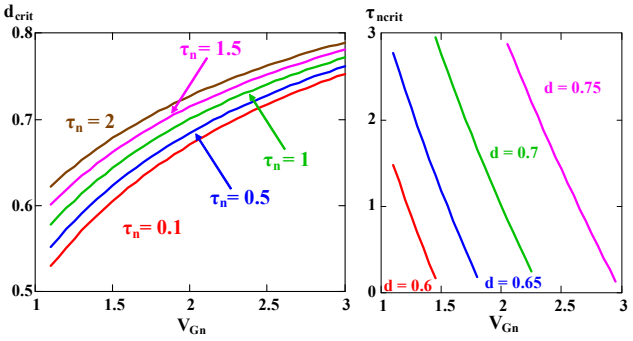

Fig. 7. Boundary between conduction modes for the DL//L LED driver. (a) d_{crit} versus V_{Gn} and τ_n. (b) τ_n versus d and V_{Gn}.

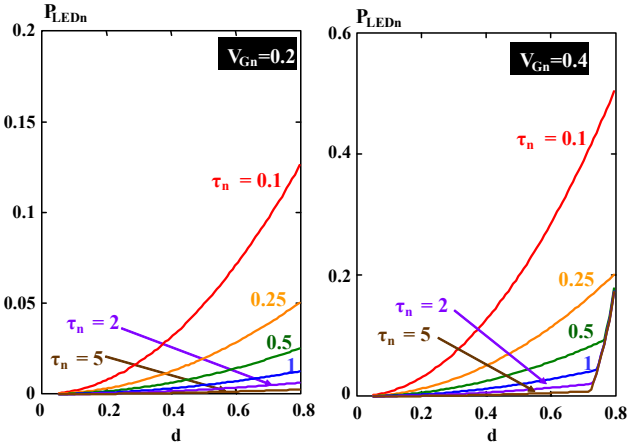

Fig. 8. Normalized average power consumed by the LED in the DL//L LED driver for different values of V_{Gn}, d and τ_n.

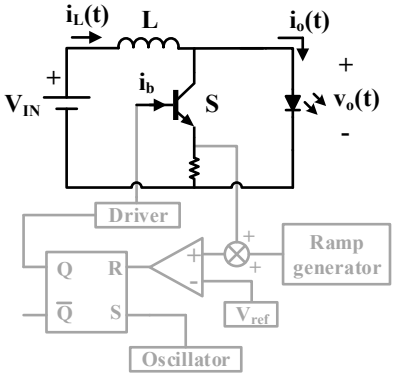

Fig. 9. Proposed control for the AC-LED drivers under study, particularized for the DL//S AC-LED driver.

sets the peak value of the current. By varying V_{ref} it is possible to achieve dimming on the LED, considering that by controlling the peak current the duty cycle on the main switch is also being controlled. In addition to its simplicity, the use of a PCMC provides not only the ability to control the current across the LEDs, but it also inherently protects both the main switch and the LED.

The previous paragraphs develop the idea of controlling the converter with a well-known and massively used control

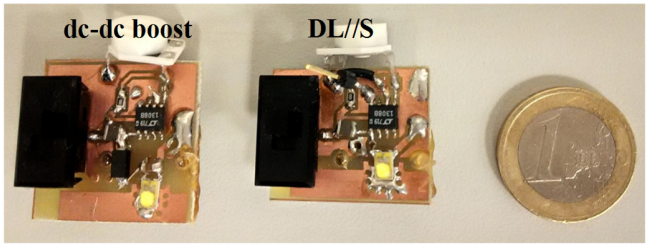

(a)

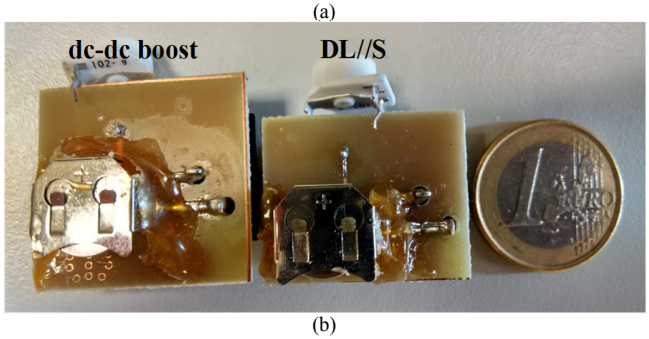

(b)

Fig. 10. Experimental prototypes of the conventional dc-dc LED boost and DL//S AC-LED driver. (a) Top layer. (b) Bottom layer.

methodology. The other problem that remains is being able to provide enough voltage from such a low input without penalizing the efficiency of the LED driver. Fortunately, this problem has been solved for single-cell Li-Ion chargers, normally by utilizing the boosted output voltage as a mean to drive the required components [17]. Therefore, there are a handful of integrated circuits that can be used for this task, as the one that will be used along the next section, which is the LT1308B [18].

IV. Experimental Results

In order to validate the analysis introduced in the previous section, two prototypes of the DL//S AC-LED driver have been designed and experimentally tested. The first prototype was designed to validate the analysis in terms of operating modes, whereas the second has been designed aiming for a compact and final design using a Li-Ion battery as its main source including the proposed control, see Fig. 10. The first prototype works in the range of 1 to 2 V, switching at 100 kHz and feeding a W42180T LED (V_{γ_LED} = 2.8 V and r_{LED} = 1.2 Ω). The first analysis is carried out in terms of the boundaries between CCM and DCM. Therefore, for d equal to 0.5 and τ_n equal to 1, Fig. 11 shows the transition between modes when the input voltage of the DL//S AC-LED driver is varied. In fact, by using Fig. 4 (a) considering the aforementioned d and τ_n, it is simple to observe that for value of V_{Gn} below 0.6 the driver should work in DCM. This value coincides with the experimental results, as Fig. 11 (a) shows the correct operation in DCM for V_{Gn} equal to 0.43 and Fig. 11 (b) shows the operation in a point considered close to critical conduction mode for a V_{Gn} equal to 0.57.

In order to complete the analysis of operating modes, Fig. 12 shows the variation of τ_n for fixed values of V_{Gn} and d. It correctly demonstrates the expected performance shown in Fig. 4 (b), in which for d equal to 0.5 at a V_{Gn} of 0.57, those values of τ_n below 1 make the AC-LED driver to operate in DCM. In contrast, values of τ_n higher than one make the AC-LED driver

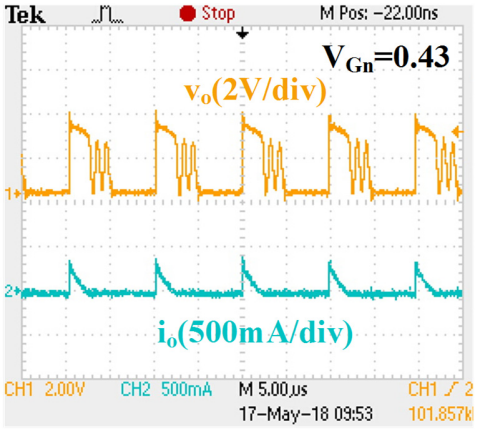

(a)

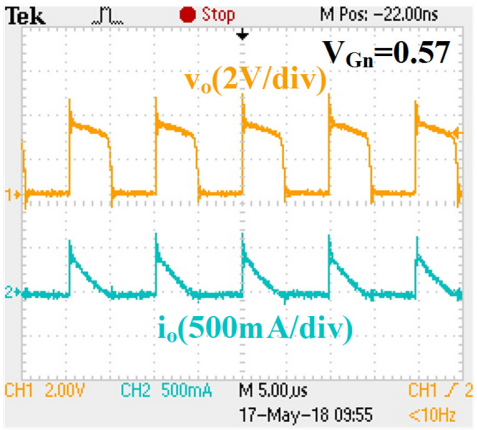

(b)

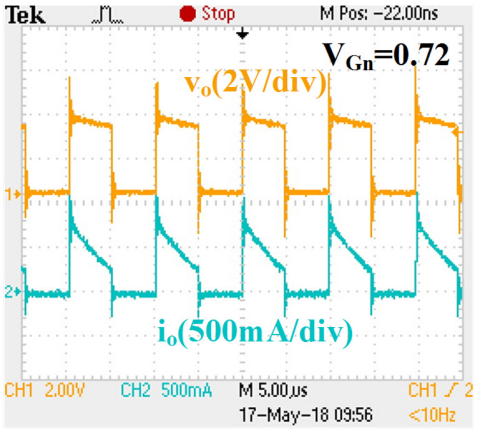

(c)

Fig. 11. Experimental waveforms of the DL//S AC-LED driver for different values of V_{Gn} while keeping d = 0.5 and τ_n = 1. (a) V_{Gn} = 0.43. (b) V_{Gn} = 0.57. (c) V_{Gn} = 0.72.

to operate in CCM. Furthermore, Fig. 13, shows the operation of the DL//S AC-LED driver for different values of d while keeping the other two parameters at a constant value.

It is important to note that the operation in CCM causes the reverse recovery phenomenon to occur [13], as can be observed in Fig. 11 (c), Fig. 12 (b) and Fig. 13 (b). In contrast, DCM

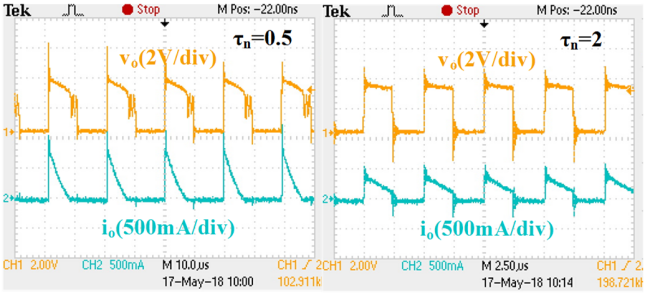

(a) (b)

Fig. 12. Experimental waveforms of the DL//S AC-LED driver for different values of τ_n while keeping d = 0.5 and V_{Gn} = 0.57. (a) τ_n = 0.5. (b) τ_n = 2.

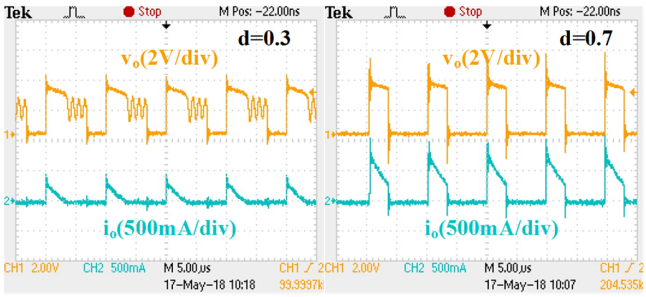

(a) (b)

Fig. 13. Experimental waveforms of the DL//S AC-LED driver for different values of d while keeping τ_n = 1 and V_{Gn} = 0.57. (a) d = 0.3. (b) d = 0.7.

operation does not show this effect due to the zero current switching towards the turn off. However, this operation in DCM will limit the maximum power given to the LED due to the higher peak current when compared with the same average current in CCM. In addition, as has been already mentioned DCM operation is not as efficient when it comes to the amount of power transferred to the LED.

Nonetheless, as has been studied in [11] and [12], the reverse recovery effect affects LEDs negatively influencing their lifetime, reason for which it is required to eliminate it. In particular, these works tackled its removal by mildly increasing the complexity of the control stage and adding an inductance. Precisely for the case under study, cost and practicality are of utter importance, reason for which the operation in DCM is attractive even if it limits the efficiency or the maximum out power of the AC-LED driver.

For the aforementioned reasons the second prototype is built to demonstrate is compactness, and is designed to operate in boundary conduction mode at the maximum power. In fact, in order to reduce the stress of the peak current across the LED the duty cycle is maximized by selecting it as the first duty curve that crosses the line of V_{Gn} in nominal conditions in Fig. 4 (b). Then, it is compared to a conventional dc-dc boost converter LED driver, which is also shown in Fig. 5. The characteristics of the DL//S AC-LED driver and the conventional dc-dc boost LED driver are similar with an input voltage varying from 1 to 2 V, a switching frequency of 600 kHz, an inductance of 1.2 µH and driving an LXML-PWC2 LED (V_{γ_LED} = 2.6 V and r_{LED} = 0.5 Ω). The main difference between the prototypes is that the

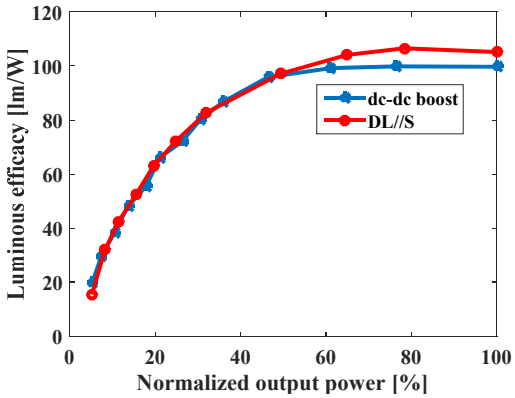

Fig. 14. Luminous efficacy versus normalized output power for the dc-dc boost LED driver and the DL//S AC-LED driver.

conventional dc-dc boost LED driver requires the use of an ultra-low forward voltage Schottky diode (UPS115Ue3), whose cost is similar to that of the LED, and an output capacitor. These two elements would significantly increase the cost of this solution, as both converters will require the same IC to perform the driving from very low input voltages (i.e., LT1308B).

In order to perform a fair comparison between the DL//S AC-LED driver and the conventional dc-dc boost LED driver, Fig. 14 shows the measured luminous efficacy of both LED drivers, when varying the output power while keeping V_{Gn} and τ_n constant at 0.57 and 1.44, respectively. The light is measured with the help of a light to volt converter based on a transimpedance amplifier (i.e., TSL-257), and then converted to lm/W in accordance. As can be seen, the luminous efficacy is similar for the lower output power values and becomes higher for the proposed topology at the higher output power values due to the voltage drop of the rectifier diode and losses. This validates not only the cost efficiency of the proposed AC-LED driver, but it also shows an advantage in terms of the outputted light per watt.

As regards the DL//L AC-LED driver, the experimental analysis carried out for the DL//S AC-LED driver is rather similar when it comes to understanding the boundaries between modes and its design. The only comment that should be added in its design is the fact that the LEDs will need to withstand negative voltages. This is an undesired performance, but considering this voltage never surpasses the knee-voltage it is safe to consider its operation in accordance to [19]. Nonetheless, it will still depend on the characteristics set by the manufacturer for the selected LED.

V. Conclusions

This paper tackles the driving of LED from very low voltages by using them as the rectifier of conventional dc-dc converters, becoming an AC-LED driver. The analysis undergone in this work renders two new topologies; one of them has been experimentally tested showing promising results in terms of luminous efficacy while reducing the cost of a conventional dc-dc converter that disposes of the Schottky diode and the output capacitance. The proposed control based on current programmed control is simple, protects both the main switch and the LED, and reduces the amount of components

required, as it is already included within the selected IC. In addition, the selected IC solves the main problem of driving an LED from very low voltages, as it already includes all the necessary circuitry to generate the auxiliary voltages to drive the main switch of the LED driver. Thus, being able to drive a single LED from a single Li-Ion battery of 1.2 V.

REFERENCES

[1] M. Arias, A. Vazquez, and J. Sebastian, "An overview of the AC-DC and DC-DC converters for LED lighting applications," Automatika—J. Control, Measure., Electr., Comput. Commun., vol. 53, pp. 156–172, 2012.

[2] Y. Chen, C. Chang and P. Yang, "A novel constant current control circuit for a primary-side controlled AC-DC LED driver," 2014 11th International Conference on Electronics, Computer and Computation (ICECCO), Abuja, 2014, pp. 1-4.

[3] John E. Bohan, Jr., "Low voltage driven oscillator circuit", U.S. patent 4 734 658A, March 29, 1988.

[4] Z. Kaparnik, "One Volt LED – A Bright Light", Everyday Practical Electronics (EPE) magazine, November 1999.

[5] J. Yang, et al. "A universal-input high-power-factor LLC resonant driver without electrolytic capacitor for PWM dimming LED lighting application," 2014 International Power Electronics and Application Conference and Exposition, Shanghai, 2014, pp. 1473-1478.

[6] B. G. Kang, Y. Choi and S. K. Chung, "High frequency AC-LED driving for street light," 2015 9th International Conference on Power Electronics and ECCE Asia (ICPE-ECCE Asia), Seoul, 2015, pp. 1246-1251.

[7] C. L. Kuo, T. J. Liang, K. H. Chen and J. F. Chen, "Design and implementation of high frequency AC-LED driver with digital dimming," Proceedings of 2010 IEEE International Symposium on Circuits and Systems, Paris, 2010, pp. 3713-3716.

[8] K. H. Loo, Y. M. Lai and C. K. Tse, "Design and Analysis of LCC Resonant Network for Quasi-Lossless Current Balancing in Multistring AC-LED Array," in IEEE Transactions on Power Electronics, vol. 28, no. 2, pp. 1047-1059, Feb. 2013.

[9] J. C. W. Lam and P. K. Jain, "A High Power Factor, Electrolytic Capacitor-Less AC-Input LED Driver Topology With High Frequency Pulsating Output Current," in IEEE Transactions on Power Electronics, vol. 30, no. 2, pp. 943-955, Feb. 2015.

[10] M. A. Juárez, P. R. Martínez, G. Vázquez, J. M. Sosa and M. Ponce, "Analysis and design for self-oscillating LED driver with high frequency pulsating output current," IECON 2015 - 41st Annual Conference of the IEEE Industrial Electronics Society, Yokohama, 2015, pp. 003992-003996.

[11] I. Castro, S. Lopez, K. Martin, M. Arias, D. G. Lamar and J. Sebastian, "High frequency dc-dc AC-LED driver based on ZCS-QRCs," 2017 IEEE Energy Conversion Congress and Exposition (ECCE), Cincinnati, OH, 2017, pp. 3688-3695.

[12] I. Castro, S. Lopez, K. Martin, M. Arias, D. G. Lamar and J. Sebastian, "A family of high frequency AC-LED drivers based on ZCS-QRCs," in IEEE Transactions on Power Electronics, vol. PP, no. 99, pp. 1-1.

[13] P. Haaf, and J. Harper. "Understanding diode reverse recovery and its effect on switching losses.", 2007.

[14] M. M. Jovanovic, "A technique for reducing rectifier reverse-recovery-related losses in high-power boost converters," in IEEE Transactions on Power Electronics, vol. 13, no. 5, pp. 932-941, Sep 1998.

[15] S. Cuk and R. D. Middlebrook, "A general approach to modeling switching dc-to-dc converters in discontinuous conduction mode". IEEE PESC 1977, pp.36-52.

[16] R. Redl and N. O. Sokal, "Current-mode control, five different types, used with the three basic classes of power converters: Small-signal AC and large-signal DC characterization, stability requirements, and implementation of practical circuits," 1985 IEEE Power Electronics Specialists Conference, Toulouse, France, 1985, pp. 771-785.

[17] R. K. Williams, B. Mohandes and Chae Lee, "High-frequency DC/DC converter for lithium-ion battery applications utilizes ultra-fast CBiC/D process technology," Applied Power Electronics Conference and Exposition, 1995. APEC '95. Conference Proceedings 1995., Tenth Annual, Dallas, TX, 1995, pp. 322-332 vol.1.

[18] "High Current, Micropower Single Cell, 600kHz DC/DC Converters", Linear Technology, Linear Technology, 2 pp. 1996, 97 Linear Technology.
[Online] http://www.analog.com/media/en/technical-documentation/data-sheets/1308abfb.pdf

[19] "Cree® XLamp® LED Electrical Overstress," Appl. Note CLD-AP29 REV 1E, Cree, Inc., Durham, NC, USA, 2016.